Geomechanics and Engineering, *Vol. 16, No. 4 (2018) 363-373*
DOI: https://doi.org/10.12989/gae.2018.16.4.363

THM analysis for an in situ experiment using FLAC3D-TOUGH2 and an artificial neural network

Sangki Kwon*[1] and Changsoo Lee[2a]

[1]*Department of Energy Resources Engineering, Inha University, Yong-Hyun dong, Namgu, Incheon, Republic of Korea*
[2]*Department of HLW disposal, Korea Atomic Energy Research Institute, Yuseong-gu, Daejeon, Republic of Korea*

(Received March 20, 2018, Revised June 12, 2018, Accepted July 16, 2018)

Abstract. The evaluation of Thermo-Hydro-Mechanical (THM) coupling behavior is important for the development of underground space for various purposes. For a high-level radioactive waste repository excavated in a deep underground rock mass, the accurate prediction of the complex THM behavior is essential for the long-term safety and stability assessment. In order to develop reliable THM analysis techniques effectively, an international cooperation project, Development of Coupled models and their Validation against Experiments (DECOVALEX), was carried out. In DECOVALEX-2015 Task B2, the in situ THM experiment that was conducted at Horonobe Underground Research Laboratory(URL) by Japan Atomic Energy Agency (JAEA), was modeled by the research teams from the participating countries. In this study, a THM coupling technique that combined TOUGH2 and FLAC3D was developed and applied to the THM analysis for the in situ experiment, in which rock, buffer, backfill, sand, and heater were installed. With the assistance of an artificial neural network, the boundary conditions for the experiment could be adequately implemented in the modeling. The thermal, hydraulic, and mechanical results from the modeling were compared with the measurements from the in situ THM experiment. The predicted buffer temperature from the THM modelling was about 10℃ higher than measurement near by the overpack. At the other locations far from the overpack, modelling predicted slightly lower temperature than measurement. Even though the magnitude of pressure from the modeling was different from the measurements, the general trends of the variation with time were found to be similar.

Keywords: THM; neural network; waste disposal; underground research laboratory; in situ experiment

1. Introduction

The evaluation of coupling behaviors between thermal load, fluid flow, and stress change is an important task in many rock engineering fields, such as the geological disposal of radioactive wastes, geothermal energy, CO_2 sequestration, deep underground mines, and conventional as well as unconventional oil and gas production. In the countries considering the geological disposal of high-level radioactive waste (HLW), a multi-barrier system consisting of natural barrier and engineered barriers is applied for ensuring the long-term safety of the repository. Rock mass is the natural barrier and canister, buffer, backfill, and concrete plug are the components of engineered barriers. A performance assessment of the disposal system needs a long-term prediction of thermal, hydraulic, mechanical, and chemical behaviors of the multi-barriers. It is, therefore, an important topic to develop techniques of coupled thermo-hydraulic-mechanical (THM) analysis in high temperature, high rock stress, and high water pressure context such as expected in an underground repository, which will be normally located at several hundred meters deep underground (Tsang *et al.* 2012). A general review of the THM coupled processes expected in HLW repositories was given by Hudson *et al.* (2005).

In the last decades, lots of efforts had been given for the development of THM analysis techniques. Some commercial codes such as COMSOL, OpenGeySys, ABAQUS, FLAC, and etc. could be used as all-in-one solutions. In some cases, integration of different codes was found to be more efficient to simulate the complex THM coupling behaviors. Table 1 lists various approaches for THM coupling applied to different fields.

For developing a reliable THM coupling technique, it is essential to validate it with in situ or laboratory experiments. In order to develop reliable THM coupling techniques validated with in situ or laboratory experiments, an international cooperative project DECOVALEX was started in 1992. During the past decades, many in situ and laboratory tests had been modeled to enhance the reliability of THM coupling techniques in different phases (Hudson and Jing 2013). The recent phase of DECOVALEX-2015 was completed in 2015 and DECOVALEX-2019 was launched.

In this study, as a part of DECOVALEX-2015, THM coupling analysis using FLAC3D-TOUGH2 was carried out for the in situ heater experiment at Horonobe URL in Japan. The experiment was designed for investigating the complex THMC behaviors of the engineered barriers and natural barrier.

Recently, new approaches utilizing an artificial neural

∗Corresponding author, Professor
E-mail: kwonsk@inha.ac.kr
[a]Ph.D.
E-mail: leecs@kaeri.re.kr

ISSN: 2005-307X (Print), 2092-6219 (Online)

Table 1 Codes used for THM coupling analysis

Projects	Codes	References
CO_2 sequestration	TOUGH2+FLAC OpenGeoSys STOMP+ABAQUS TOUGH2 +CODE_ASTER ECLIPSE+ABAQUS	Rutqvist *et al.* (2010), Magri *et al.* (2012), Carroll (2011), Loschetter *et al.* (2012), Elyasi *et al.* (2016)
Coal bed methane	TOUGH2(EOS7C) TOUGH2+CODE_ASTER	Stephen (2011), Loschetter *et al.* (2012)
Geothermal	OpenGeoSys +RockFlow FEHM CODE_BRIGHT TOUGH2+EGS	Watanebe *et al.* (2009), Pandey *et al.* (2017), Olivella *et al.* (1996), Hu *et al.* (2012)
Methane hydrate	FLAC TOUGH2+FLAC3D	Klar *et al.* (2010), Rutqvist *et al.* (2008)
Mining	FLAC	Yang, *et al.* (2013)
Oil sand (SAGD)	COMSOL EXOTHERM+FLAC VISAGE/ECLIPS Pumaflow+ABAQUS	Gong and Wan (2008), Li and Chalaturnyk (2005), Khan *et al.* (2011), Guy *et al.* (2013)
Radioactive waste	TOUGH2+FLAC3D OpenGeoSys+Rockflow CODE_BRIGHT	DOE (2012), Kwon (2013), Yildizdag (2010), Li *et al.* (2013)
Shale gas	FRACMAN	Dershowitz *et al.* (2011)
Underground space	CODE_BRIGHT	Gesto *et al.* (2013)

network have been reported for more reliable and efficient computer simulations. Kwon *et al.* (2013) reported that the application of an artificial neural network (ANN) was useful for stepwise submodeling. Shahrbanouzadeh *et al.* (2015) performed a simulation of flow through dam foundation using finite element (Seep3D) and ANN. In this study, an ANN was applied to implement the measured temperatures from the in situ heater experiment as the boundary conditions in the modeling for more accurate calculation.

2. In situ experiment at Horonobe URL

An in situ experiment for investigating the THM behaviors of rock and engineered barriers including bentonite buffer, backfill, concrete plug, and concrete lining under the HLW repository conditions was prepared in full scale at Horonobe Underground Research Laboratory (URL) by Japan Atomic Energy Agency (JAEA). Horonobe URL is located in Wakanai, Hokaido, Japan. The in situ experiment is to simulate the THM behaviors in the HLW disposal concept of Japan, which was reported in the H12 report (JNC 2000). According to the H12 report, the

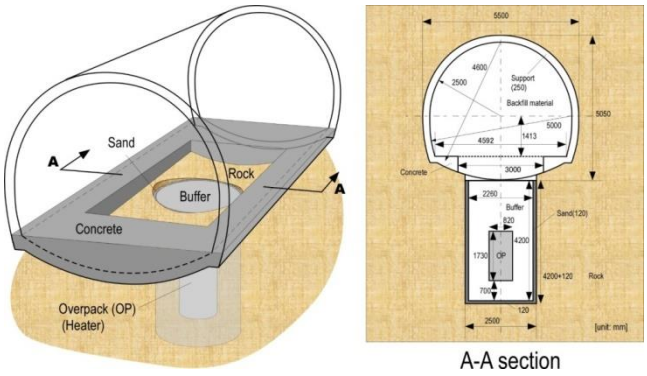

Fig. 1 Layout of the Horonobe EBS experiment (Sugita *et al.* 2015)

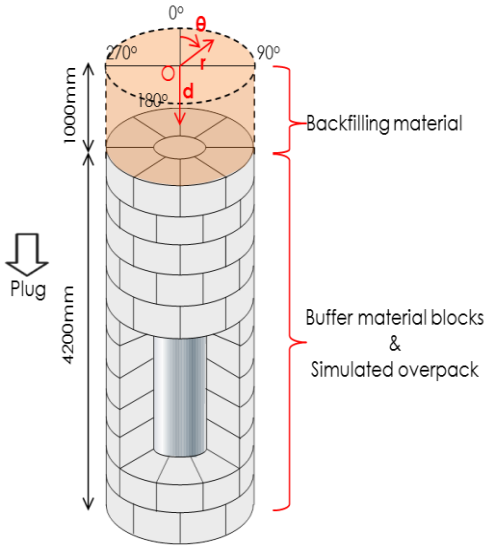

Fig. 2 Layout of the buffer, overpack, and backfill and the parameters influencing on overpack temperature (Sugita *et al.* 2015)

vitrified HLW will be disposed, several hundred meters deep underground, after emplacing in cast iron overpacks. The gap between the overpack and rock will be filled with tens of cm thick buffer, which will be made of the mixture of bentonite and sand. The in situ experiment was started in 2015. Fig. 1 shows the layout of the in situ experiment. The test tunnel of size 5 m × 5.5 m is located at 350 m deep underground. The diameter of the vertical emplacement hole drilled in the floor is 2.5 m. The overpack's diameter is 0.82 m. The thickness of the buffer layer surrounding the overpack is 0.7 m-0.72 m. There is a 12 cm thick sand layer between buffer and rock. The test tunnel is supported by a concrete lining and a concrete plug is installed to seal the test area.

Fig. 2 shows the layout of the buffer, overpack, and backfill. For the in situ experiment, various sensors were installed to measure the thermo-hydro-mechanical behaviors. Table 2 lists the information of the sensors installed for the THM experiment. Ten thermocouples were installed on the surface of the overpack. Fig. 3 shows the temperature variation measured from the thermocouples. The measured temperatures were used as the thermal

Table 2 Sensors installed for the in situ THM experiment (Sugita *et al.* 2015)

Sensor	ID	r(mm)	θ(°)	d (mm)
Piezometer	PP001	955	90	5,200
	PP002	605	270	
	PP003	955	270	
	PP004	1165	123.75	
Borehole extensometer	DS001-1	200	337.5	4,850
	DS002-1	780	337.5	
Borehole extensometer	DS001-2	200	337.5	
	DS002-2	780	337.5	
Borehole extensometer	DS002-3	780	337.5	4,150
Pressure cell	TP008	517.5	11.25	3,450
	TP009	605	0	
	TP010	867.5	11.25	
	TP011	955	0	
Borehole extensometer	DS02-4	780	337.5	
Thermocouple in the buffer	TE007	605	45	
	TE008	780	45	
	TE009	955	45	
Borehole extensometer	DS002-5	780	337.5	3,100
Psychrometer	PS009	955	315	
Borehole extensometer	DS002-6	780	337.5	2,050
Thermocouple of the simulated overpack	TEOP001	205	270	4,500
	TEOP002	410	90	4,150
	TEOP003	410	270	4,150
	TEOP004	410	90	3,625
	TEOP005	410	270	3,625
	TEOP006	410	0	3,450
	TEOP007	410	180	3,450
	TEOP008	410	90	3,100
	TEOP009	410	270	3,100
	TEOP010	205	270	2,750

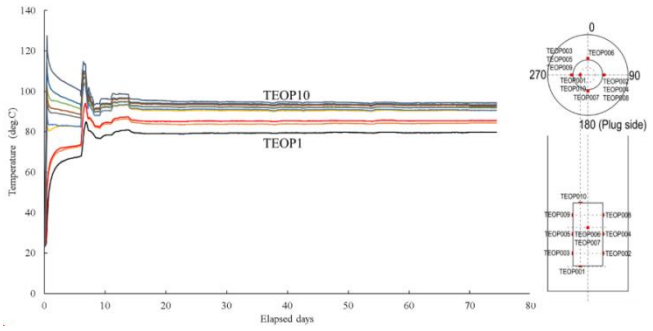

Fig. 3 Measured overpack temperatures (Sugita *et al.* 2015)

boundary conditions in the computer simulation carried out in this study.

Normally, the maximum buffer temperature is required to be maintained lower than 100℃ in order to prevent possible loss of capability of buffer material, which may be induced by certain chemical variation in minerals in high temperature condition. The prediction of THM behaviors in the in situ experiment was the topic of Decovalex-2015 Task B2, in which five research teams including BGR (Germany), CAS (China), DOE-LBNL (USA), KAERI-Inha University (Korea) and JAEA (Japan) were participated.

3. THM coupling method

3.1 FLAC3D-TOUGH2 coupling

TOUGH2 is a general-purpose numerical simulation program for multi-dimensional fluid and heat flows of multiphase, multi-component fluid mixtures in porous and fractured media (Pruss *et al.* 1999). It has been applied to a wide range of problems in heat and moisture transfer, and in the drying of porous materials. FLAC3D is a well-known and widely used commercial geo-mechanical code developed by Itasca consulting group (Itasca 2011). Since FLAC3D possesses a variety of options for mechanical analysis under different conditions, it can cover the deficient mechanical calculation capacity in TOUGH2.

By linking the codes TOUGH2 and FLAC3D, coupled thermo-hydraulic-mechanical (THM) processes can be performed for investigating multiphase flow in rock masses or other geological media under various stress conditions. The technique for linking between TOUGH2 and FLAC3D code was developed by Rutqvist and Tsang (2002, 2003). The combined TOUGH2-FLAC3D simulator has been successfully applied to various projects for radioactive waste disposal, geothermal operation, CO_2 storage in geological formation, hydrate sediment, etc. (Rutqvist *et al.* 2010, Rutqvist 2011).

In this study, a TOUGH2-FLAC3D coupling analysis technique with an artificial neural network (ANN) routine was developed. Fig. 4 shows the calculation flow for the THM analysis using the two codes. TOUGH2 was used for thermal-hydraulic (TH) analysis, while FLAC3D was used for thermal-mechanical(TM) analysis. TOUGH2/EOS3 (Equation Of State 3) module for the multi-phase and multi-component analysis of water and air flow was used for the hydraulic analysis. The TOUGH2/EOS3 module, fluid flow is governed by a multiphase extension of Darcy's law (Hu *et al.* 2013). In the mechanical analysis, Mohr-Coulomb failure criterion was used for calculating elastic-perfectly plastic deformation. Heat conduction was only considered in the thermal analysis. The results such as saturation(S) and pressure (P) from TH were exported as input files to define the initial condition in FLAC3D. The results such as porosity(φ), temperature(T), and permeability(K) from TM analysis were exported to define the initial condition in TOUGH2. Such a sequential exchange of calculation results was carried out with adequate time interval, which was 1 day, in this study. The reason to perform thermal calculation again in FLAC3D is that the variation in water content in rock and buffer can change the thermal and mechanical

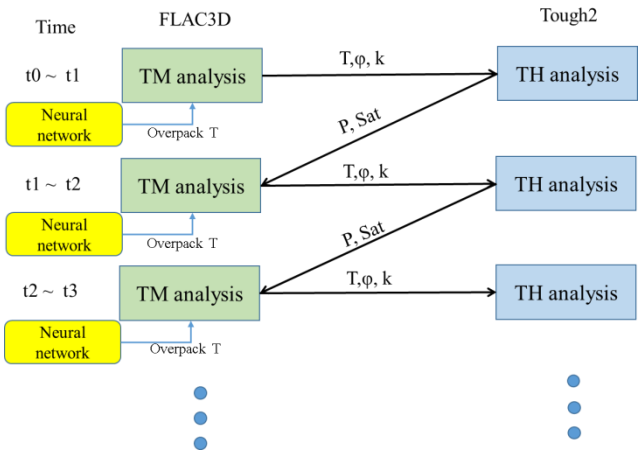

Fig. 4 Flow of THM coupling analysis using TOUGH2 and FLAC3D and neural network

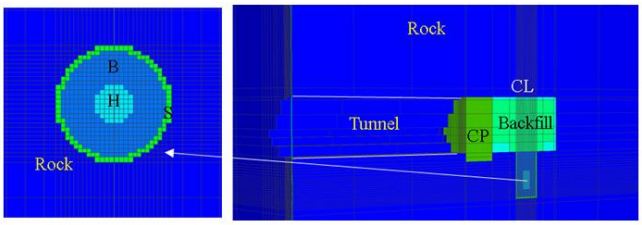

Fig. 5 Model mesh for three-dimensional THM analysis (B: buffer, H: overpack, S: sand, CP: concrete plug, CL: concrete lining)

properties of the materials. Thermal and mechanical analysis with the changed properties can result in different temperature distribution from TH analysis. By implementing the temperatures calculated from FLAC3D as an initial condition in TOUGH2 in the next step, the temperature difference could be adjusted. For more accurate simulation, the measured overpack temperatures at different measuring points were used as boundary conditions. In order to implement the temperature boundary conditions as close to the actual measurements as possible, a new way using ANN based on backpropagation learning algorithm was developed.

Fig. 5 shows the 3D model mesh used in this study. About 45,000 zones were allocated for considering backfill, concrete lining, concrete plug, open tunnel as well as the 12 cm thick sand layer surrounding the buffer.

3.2 Artificial neural network

Artificial neural networks (ANN) are computer algorithms, which have the capacity to learn the relationships between input and output parameters. ANNs had already been applied in various areas for prediction, classification, pattern recognition, etc. It needs learning or training process from previous experiences. During the learning process, the error between the desired or known output and the predicted output from the network should be minimized by adjusting the network(Engelbrecht 2007). Different learning algorithms can be used for training of the networks. Back-propagation (BP) is one of the most popular learning algorithms. A BP ANN consists of a number of

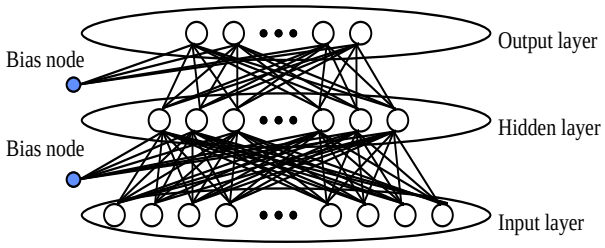

Fig. 6 Structure of artificial neural network

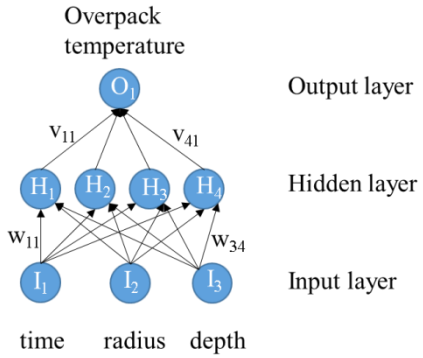

Fig. 7 Neural network for calculating the overpack temperatures as boundary conditions

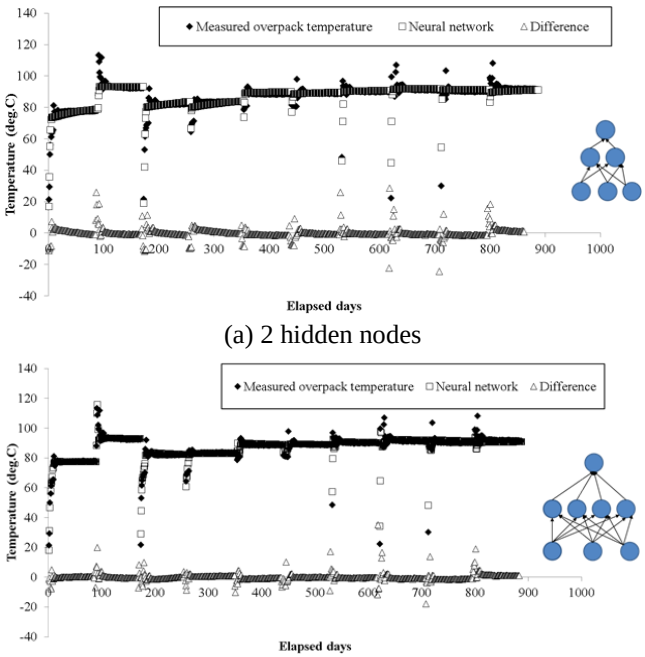

(a) 2 hidden nodes

(b) 4 hidden nodes

Fig. 8 Measured overpack temperatures and calculated temperatures from neural network after training

neuron-containing layers. The neurons in input and hidden layers and hidden and output layers are interconnected as shown in Fig. 6. During the training of BP ANN, the weight values (w_{ij}, v_{ij}) allocated at each connection are adjusted to minimize the error.

The number of neurons in the input and output layers are the same as the number of input and output parameters. In the case of the hidden layer located in between the input

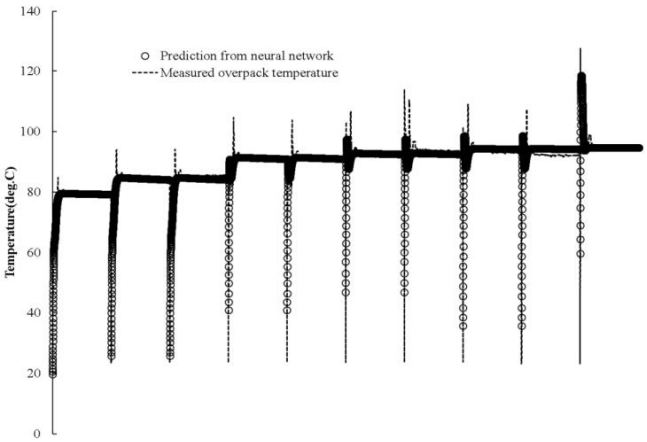

Fig. 9 Comparison of all measured overpack temperatures and calculated temperatures from the neural network for testing the network

and output layers, the adequate number of neurons needs to be determined from trial and error.

In the modelling, the measured overpack temperatures were used as boundary conditions. As listed in Table 2, ten thermocouples were installed at different locations in the overpack. As shown in Fig. 3, there are significant differences between the measured temperatures at the locations. It is, therefore, not recommended to use the average value as the boundary condition. Another problem is that it is not easy to match the measuring locations and grid points in the model.

It would be better to develop a way to calculate the temperatures, which are strongly dependent on the measuring location as well as time, and to implement them as boundary conditions in the model. In order to do that, a neural network as shown in Fig. 7 was trained and tested. The trained neural network using the measured temperature data could calculate the complex temperature variation at any locations in the overpack during the calculation time. The network was then implemented in the simulation model using a FISH program to calculate the boundary overpack temperatures.

Three neurons for depth (d), distance from center axis of overpack (r), and time (t) are in the input layer and one neuron for overpack temperature is in the output layer. In the case of hidden layer, 2 - 4 hidden neurons were tested to select the adequate number of neurons in the hidden layer. For training of the neural network, 900 measured data were randomly selected and trained. During the training, the weight values of each connection between input-hidden nodes and hidden-output nodes were adjusted until the network predicts the measured temperatures with acceptable errors. Fig. 8 shows the comparison of the temperatures measured and predicted from the network after training. Since the network with 4 hidden neurons predicted the temperatures more accurately than with 2 hidden neurons, a network with 4 hidden neurons was used in the further study. Before utilizing the trained network, it should be tested in order to check the reliability of the network. Testing of the trained network was done with 17,878 data, which were not used for training. As shown in Fig. 9, the network could successfully predict the temperatures. The average value of the measured temperature was 89.15℃, while the network predicted 89.3℃.

4. THM analysis

4.1 Material properties

The material properties of overpack, buffer, and rock in the modelling were provided in the JAEA Task B2 definition report (Sugita *et al.* 2015).

4.1.1 Parameters for buffer

Mohr-Coulomb plastic model was used for the buffer. Cohesion was set to zero and the friction angle was specified as 16.7°. Biot's constant of the buffer was set as 1.0. Thermal conductivity of the buffer (K_b) was calculated using the following equation, which was provided by JAEA for the buffer used in the in situ experiment

$$K_b = 0.444 + 0.0138w + 6.14e - 3w^2 - 1.69e - 4w^3 \quad (1)$$

where, w is gravimetric water content(%).

Initial gravimetric water content in the buffer was set as 12.5%. For the initial condition of water content of 12.5%, thermal conductivity was calculated as 1.2458 W/(m·K). In the modelling, the thermal conductivity with water content was assumed to be changed linearly from 0.44 W/(m·K) in dry condition to 2.0 W/(m·K) in fully saturated condition.

The given permeability of 4E-20 m^2 for the buffer was used in the modelling. Capillary pressure was assumed to follow the van Genuchten function, given by

$$P_c = P_o[S_e^{-1/a} - 1]^{1-a},\ P_o = \frac{1}{\lambda} \text{ and } a = 1 - \frac{1}{n} \quad (2)$$

With λ = 8E-3(1/m) and n = 1.6 as given in the JAEA report, parameters in Eq. (2) were derived as P_o = 1.22 MPa and a = 0.375. The maximum capillary pressure was assumed to be 1E7 Pa. The relative permeability of liquid was calculated by using the following equation. The value of 1.3 was determined from the back analysis of infiltration test (Sugita 2015).

$$RP_{liq} = S_l^{1.3} \quad (3)$$

where, RP_{liq} represents relative permeability of liquid, S_l is liquid saturation,

4.1.2 Parameters for rock mass

Bulk and shear modulus were calculated from given Young's modulus and poisson's ratio as 1.046 GPa and 765 MPa, respectively. Density of 1,354 kg/m^3 and porosity of 44.82% were used. Rock was assumed to be fully saturated in the initial condition. Biot's constant of rock mass was set as 1.0. Thermal conductivity of the rock mass in dry condition was 0.579 W/(m·K), while it was 1.231 W/(m·K). Initial gravimetric water content in rock mass was 33.1%. A hydraulic conductivity of 2.8E-8 m/s measured at Wakanai formation was used in the modeling. Permeability

Table 3 Material properties used in the modeling

	Properties	Buffer	Rock	Overpack
Mechanical	Model type	M-C	Elastic	Elastic
	Bulk modulus (Pa)	31.28E6	1.046E10	1.67E11
	Shear modulus(Pa)	14.43E6	0.752E10	7.69E10
	Cohesion(Pa)	0	-	-
	Friction angle	16.6	-	-
	Density(kg/m^3)	1,600	1,354	7,800
	Poisson's ratio	0.3	0.21	0.25
Thermal	Dry thermal conductivity (W/(m·K)) Wet thermal conductivity (W/(m·K))	0.44 2.0	0.579 1.231	53
	Specific heat (J/kg·K)	1,000	833	460
	Thermal expansion coeff.	1E-6	1.34E-5	1.64E-6
Hydraulic	Permeability(m^2)	4E-20	1.33E-15	-
	Porosity	0.403	0.386	0.001
van Genuchten	a	0.375	0.503	
	Po (pa)	1.22E6	0.987E6	

Table 4 Material properties of concrete, sand, and backfill

		Concrete	Sand	Backfill
Mechanical	Model type	Elastic	Elastic	M-C
	Bulk modulus (Pa)	16.7E9	5E6	5E6
	Shear modulus(Pa)	12.5E9	1E6	1.07E6
	Cohesion(Pa)	-	-	0
	Friction angle	-	-	10
	Density(kg/m^3)	2,280	1,560	1,400
	Poisson's ratio	0.2	0.4	0.4
Thermal	Dry thermal conductivity (W/(m·K))	2.56	0.789	0.337
	Wet thermal conductivity (W/(m·K))	2.56	2.73	1.408
	Specific heat (J/kg·K)	1,050	1,000	1,260
	Thermal expansion coeff.	1E-6	1E-8	1E-6
Hydraulic	Permeability(m^2)	1.021E-17	1.33E-14	1.79E-19
	Porosity	0.13	0.4	0.46
Van Genuchten	a	-	0.627*	0.375
	Po (Pa)	-	686*	1.22E6

of rock mass was calculated as 2.858E-15 m^2 with the dynamic viscosity of water of 0.001002 kg/(m·s) at 20℃. For the rock mass, the van Genuchten parameter α was given as 9,928E-3 (1/m), a = 0.503 were given by JAEA.

Table 5 Equations for material property changes during the calculation

Rock	Thermal conductivity(W/(m·K) *	0.579+0.0197w
	Specific heat (kJ/kg·K) *	(62.6+3.2w)/(100+w)
	Relative permeability*	S^4
Buffer	Thermal conductivity(W/(m·K)) *	0.444+0.0138w+6.14e-3w^2-1.69e-4w^3
	Specific heat (kJ/kg·K) *	(34.1+4.18w)/(100+w)
	Young's modulus(MPa) *	58.74-1.87w
	Relative permeability*	$S_l^{1.3}$
Sand	Thermal conductivity(W/(m·K))	$K_s^{1-\phi}K_w^{\phi s}K_a^{\phi(1-s)}$
	Relative permeability*	S^4
Backfill	Thermal conductivity(W/(m·K))	0.339+0.0297w
	Relative permeability*	$S_l^{1.3}$
Concrete	Relative permeability*	S^4

Then,

$$P_o = \frac{1}{9.928e-3} = 100.7\ \text{m} = 0.987\ \text{MPa} \quad (4)$$

The relative permeability in rock mass was calculated using Corey's function.

$$RP_{liq} = S^4,\ RP_{gas} = (1-S^2)(1-S^2) \quad (5)$$

$$S = \frac{(S_l - S_{lr})}{(1 - S_{lr} - S_{gr})} \quad (6)$$

where, RP_{gas} represents relative permeability of gas, S_l is liquid saturation, S_{lr} is relative saturation of liquid, S_{gr} is relative saturation of gas. In this modelling, $S_{lr} = S_{gr} = 0.0$. The initial capillary pressure in rock mass was zero, since the effective saturation was 1.0.

4.1.3 Parameters for overpack

An elastic modulus of 200 GPa and a Poisson's ratio of 0.3 were specified in JAEA report and were used. Thermal conductivity of 53 W/(m·K), specific heat of 460 J/kg·K, and thermal expansion coefficient of 1.64E-6 were used. Since it can be assumed that there is no groundwater flow through the overpack, extremely low permeability was allocated. As mentioned before, the measured overpack temperatures at different locations were used as the boundary condition.

4.1.4 Parameters for other materials

The properties of backfill were from JAEA report. In the case of sand, the mechanical and hydraulic properties were assumed from the properties of rock, buffer and backfill. Thermal conductivity of sand (K_{sand}) was calculated using geometric mean of the thermal conductivity of soild(K_s), water(K_w), and air(K_a).

$$K = K_s^{1-\emptyset} K_w^{\emptyset S} K_a^{\emptyset(1-S)} \quad (7)$$

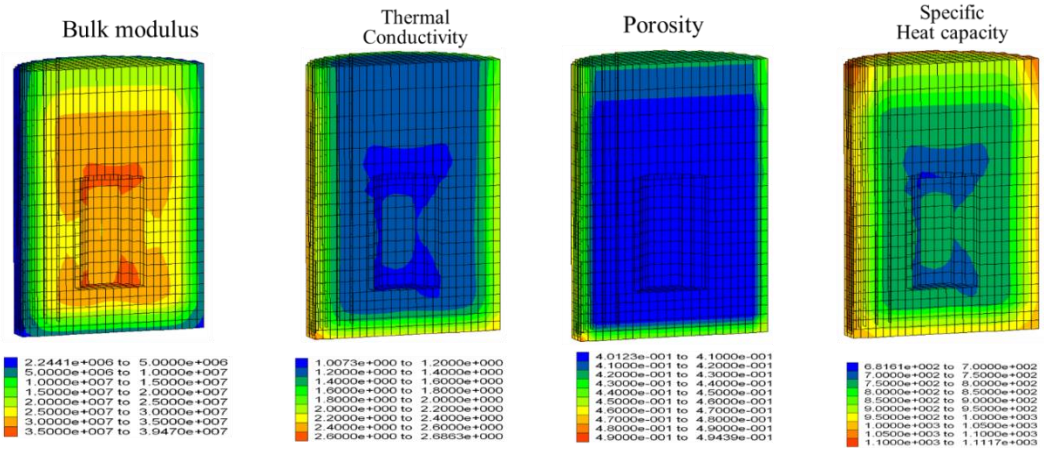

Fig. 10 Distribution of rock properties in buffer at 100 days after heating

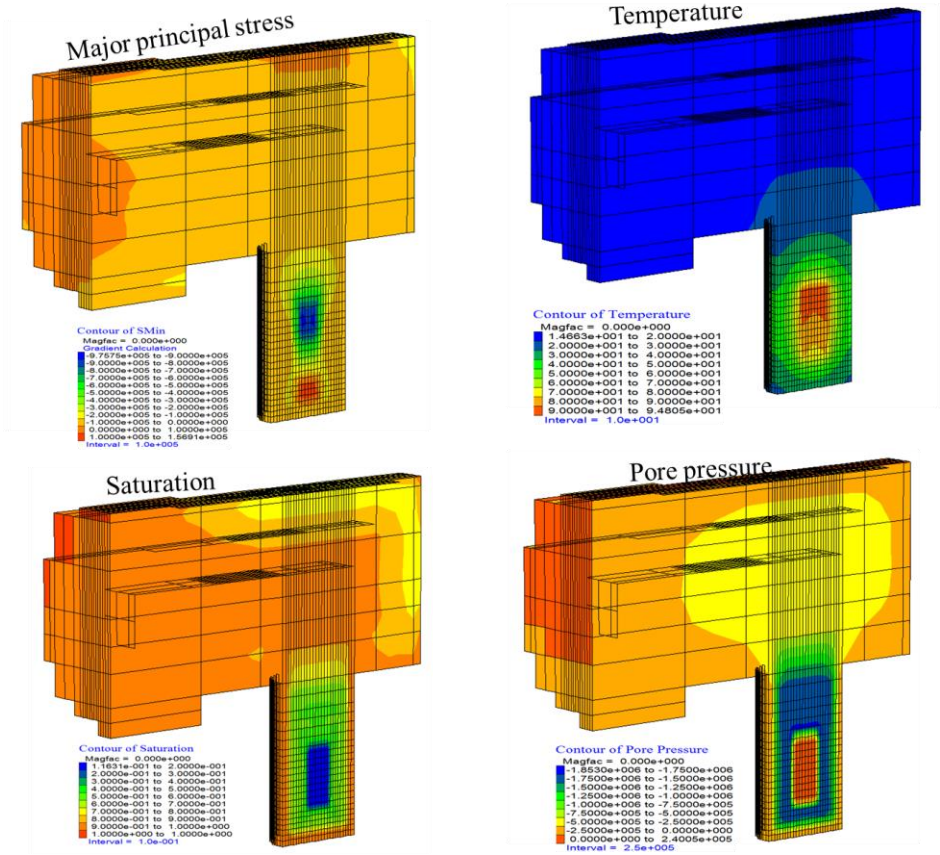

Fig. 11 Calculated results from THM coupling analysis at 100 days after heating

where, ∅ is porosity and S is saturation of water. The typical quartz, air, and water thermal conductivities, 7.69 W/(m·K), 0.026 W/(m·K), and 0.58 W/(m·K), respectively, were used in the calculation.

Table 3 summarizes the material properties used in the modelling; isotropic material properties were assumed. The material properties of concrete, sand, and backfill are listed in Table 4. Table 5 shows the equations for implementing the material property change with water content variation.

Asterisk (*) marked properties were continuously changed during the calculation.

4.2 Modeling condition

The following are the initial conditions for the modelling.

- Initial temperature: 15 ℃
- Heater temperature change with time
- Saturation of buffer: 50%
- Saturation of rock: 100%
- Saturation of sand: 100%
- Materials: rock, buffer, overpack, sand, backfill, concrete lining, concrete plug

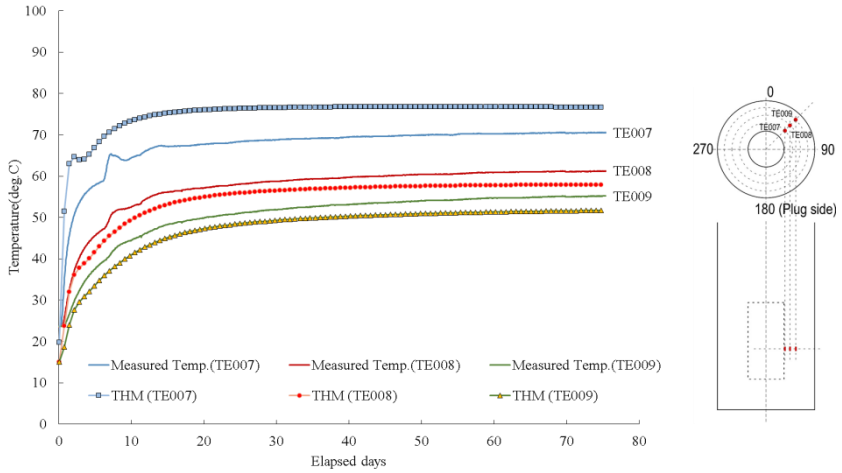

Fig. 12 Comparison of measured and calculated temperatures at different locations

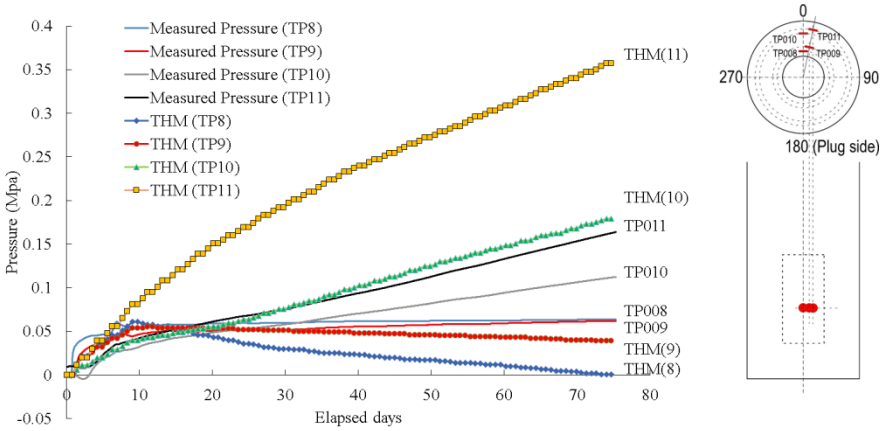

Fig. 13 Comparison of pressure change with time at different locations

• Constant temperature boundary
• Half model with fixed boundary

Some information, especially, for backfill and sand were missing; resulting in the use of several assumptions as followings;

- *Backfill*
• Initial water content: 30% (91% of saturation)
• Initial thermal conductivity: 1.3116(W/m·K) with 91% saturation
• Thermal expansion: 1/100 of buffer
• Initial pore pressure: 2.2E5
- *Sand*
• Permeability: 10 times higher than rock
• Thermal conductivity: geometric mean of thermal conductivity of solid, water, and air
• Initial pore pressure: 2.2E5
• Thermal expansion coefficient: same as backfill
• Elastic modulus: same as backfill

Direchlet boundary conditions, with which extremely large volume was allocated in the boundary elements, were applied for simulating the fixed thermal and hydraulic boundary conditions.

4.3 Results from THM analysis

Fig. 10 shows the distribution of bulk modulus, thermal conductivity, porosity, and specific heat capacity in buffer at 100 days after heating. The material properties were changed with time due to the variation of water content. As expected, the buffer near the rock shows lower bulk modulus and higher thermal conductivity and specific heat than initial values due to the increase of water content with time.

Fig. 11 shows the stress, temperature, saturation, and pore pressure distributions at 100 days after heating. The pore pressure (P_P) initialized in FLAC3D was calculated using the gas pressure (P_g) and liquid pressure (P_l) from TH analysis using TOUGH2.

$$P_P = S_g \times P_g + S_l \times P_l \quad (7)$$

where, S_g is the gas saturation and S_l is the liquid saturation. Relatively higher compressive stress of 1MPa might be related to the thermal expansion of the overpack toward the tunnel floor with the increase of temperature. The lower temperature in the lower part of the buffer can be explained with the fact that the thermal conductivity of sand, which is located below the buffer, is higher than that of buffer and backfill. Saturation and pore pressure were changed from the outer buffer zone due to the inflow of groundwater from the rock.

Fig. 12 shows the comparison of measured and calculated temperatures at 3 locations, TE007, TE008, and

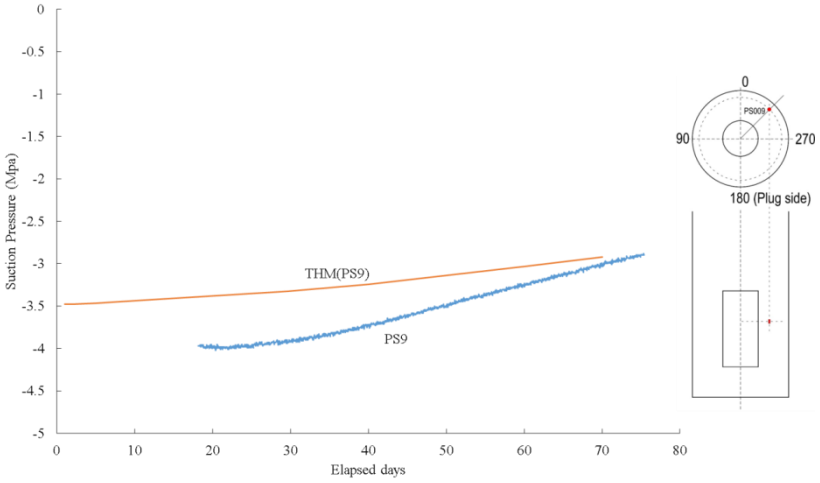

Fig. 14 Comparison of suction pressure at PS9

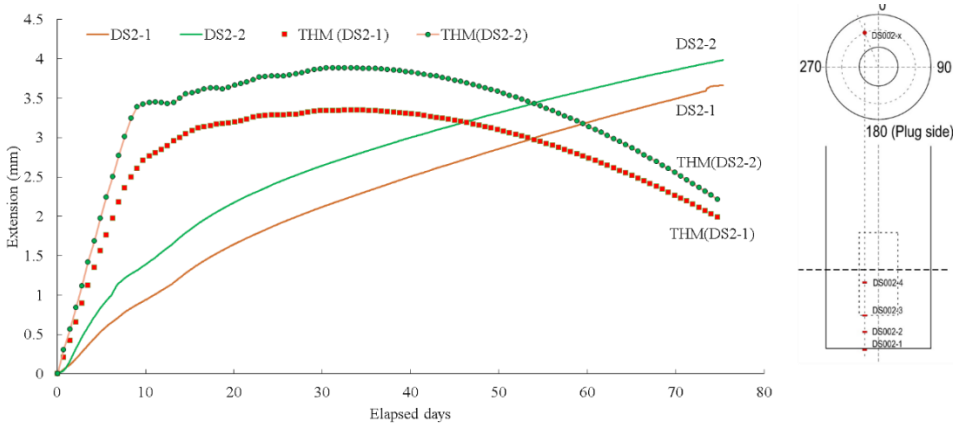

Fig. 15 Comparison of extension at different locations

TE009 installed in the buffer. In the case of TE007, which is close to the overpack, the prediction from THM modelling was about 10 ℃ higher than measurement. At the other two locations, which are far from the overpack, modelling predicts slightly lower temperatures than the measurements. It tells the thermal conductivity of buffer implemented in modelling is lower than actual thermal conductivity. In this modelling, the thermal conductivity of buffer was updated during the modeling using Eq. (1), which shows the relationship between thermal conductivity and water content, but the possible thermal conductivity related to porosity change was not included. With the consideration of thermal conductivity adjustment with porosity change, the difference between modelling and measurement might be reduced. Fig. 13 shows the comparison of measured and calculated pressure at different locations. Measured pressure means the total pressure measured by using a pressure cell, while the calculated pressure means the variation of pore pressure from the initial pressure at the same location. Even though the magnitude of pressures from modelling was different from the measurements, general trend of the variation with time was similar. In the case of TP9, the trend of variation with time as well as the magnitude of pressure were quite similar to the actual measurement. Fig. 14 shows the comparison of suction pressure in the buffer at the location of psychrometer PS009. There is about 0.5MPa difference between the measurement and computer simulation in the early stage. This may yield errors in prediction in the early stage, since the suction pressure is related to the evolution of swelling pressure, swelling strain, relative humidity, etc. (Tong *et al.* 2010).

Fig. 15 shows the comparison of extension at different locations. In the early stage, the extensions at the locations were similar; in the modelling, the extensions were steadily decreased in contrast to the continuous increase in actual measurement. There are two possible explanations for the difference. The first one is elastic modulus change. The extension data showed that the elastic modulus in modelling was lower than actual elastic modulus in the early stage, but later it was higher than the actual one. Even though the elastic modulus change in actual condition might be influenced by many parameters such as water content, temperature, porosity, etc., water content was only considered to adjust the elastic modulus in the modelling. The other possible explanation is swelling pressure, which was not considered in this modelling. Usually, a saturated bentonite can produce high swelling pressure up to several MPa, depending on bentonite type and confining condition. With the consideration of the swelling pressure in

modelling, the extension in the later stage can be predicted more accurately. Further investigation is needed for more accurate prediction of deformational behaviour.

5. Conclusions

In this study, a THM coupling analysis, in which TM and TH coupling analysis were sequentially carried out using TOUGH2 and FLAC3D, was developed and applied to the in situ THM experiment carried out at Horonobe URL. Using FISH function, the material property changes related to water content could be effectively implemented. With the help of a backpropagational artificial neural network, the measured overpack temperatures could be successfully allocated as boundary conditions. With the sequential TM-TH coupling analysis, the variation of material properties including thermal conductivity, bulk modulus, permeability, and specific heat of buffer, backfill, and rock related to the variation of water content could be effectively considered in the modelling.

Temperature, pressure, and displacement could be reasonably predicted with the THM coupling analysis using TOUGH2-FLAC3D. At a measuring point close to the overpack, the predicted temperature from THM modelling was higher than the measurement, while it was slightly lower temperature than measurement at the locations far from the overpack. From that it was possible to deduce the thermal conductivity of buffer used in modelling was lower than actual thermal conductivity. The predicted pressure variation with time from modelling was similar to the measurements in general. In the case of TP9, the trend of variation with time as well as the magnitude of pressure were quite similar to the actual measurement. The predicted extensions in buffer were different from actual measurements, even though they were increased similarly in the early stage. The difference might be related to elastic modulus change, which can be influenced by many parameters such as water content, temperature, and porosity. The difference between the modelling and measurement might be improved with more precise implementation of properties and the consideration of swelling pressure expected in saturated buffer.

Acknowledgements

This work was supported by Inha University research grant (INHA 55833).

References

Carroll, K.C., Nguyen, B.N., Fang, Y., Richmond, M.C. and Murray, C.J. (2011), "Coupling of STOMP and ABAQUS for hydro-geomechanical modeling of fluid flow and rock deformation associated with subsurface CO_2 Injection", *American Geophysical Union, Fall Meeting 2011*, San Francisco,CA, USA.

Dershowitz, W., Ambrose, R., Lim, D.H. and Cottrell, M. (2011), "Hydraulic fracture and natural fracture simulation for improved shale gas development", *Proceedings of the AAPG Annual Convention and Exhibition*, Houston, Texas, U.S.A.

DOE (2012), *Report on Modeling Coupled Processes in the Near Field of a Clay Repository*, FCRD-UFD-2012-000223.

Elyasi, A., Goshtasbi, K. and Hashemolhosseini, H. (2016), "A coupled geomechanical reservoir simulation analysis of CO_2-EOR: A case study", *Geomech. Eng.*, **10**(4), 423-436.

Engelbrecht A.P. (2007), *Computational Intelligence*, John Wiley & Sons Ltd., Chichester, U.K.

Gesto, J.M., Gens, A. and Arroyo, M. (2013), "THMC modelining of jet grouting", *Proceedings of the 12th International Conference on Computational Plasticity: Fundamentals and Applications*, Barcelona, Spain, September

Gong, X. and Wan, R. (2013), "Simulation of geomechanical reservoir behavior during SAGD process using COMSOL multiphysics", *Proceedings of the 2013 COMSIL Conference*, Boston, Massachusetts, U.S.A.

Guy, N., Enchéry, G. and Renard, G. (2013), "Numerical modeling of thermal EOR: Comprehensive coupling of an AMR-based model of thermal fluid flow and geomechanics", *Oil Gas Sci. Technol.*, **67**(6), 1019-1028.

Hu, L., Winterfeld, P.H., Fakcharoenphol, P. and Wu, Y.S.(2013), "A novel fully-coupled flow and geomechanics model in enhanced geothermal reservoirs", *J. Petrol. Sci. Eng.*, **107**, 1-11.

Hudson, J.A., Stephasson, O. and Andersson, J. (2005), "Guidance on numerical modelling of thermo-hydro-mechanical coupled processes for performance assessment of radioactive waste repositories", *Int. J. Rock Mech. Min. Sci.*, **42**(5-6), 850-870.

Itasca (2011), *FLAC 7.0 User's Manual.*

Khan, S., Ansari, S., Khan, K. and Hussein, M. (2011), "Predicting wellbore stability in SAGD infill wells using 3D finite element modeling", *Proceedings of the CSPG,CSEG,CWLS Convention*, Calgary, Alberta, Canada, May.

Klar, A., Soga, K. and Ng, M.Y.A. (2010), "Coupled deformation-flow analysis for methane hydrate extraction", *Geotechnique*, **60**(10), 765-776.

Kwon, S., Lee, C., Jeon, S. and Choi, H.J. (2013), "Thermo-mechanical coupling analysis of APSE using submodels and neural networks", *J. Rock Mech. Geotech. Eng.*, **5**(1), 32-43.

Li, P. and Chalaturnyk, R.J. (2005), "Geomechanical model of oil sand", *Proceedings of the SPE International Thermal Operations and Heavy Oil Symposium*, Calgary, Alberta, Canada, November.

Li, X., Zhang, C. and Rohlig, K.J. (2013), "Simulation of THM processes in buffer-rock barriers of high-level waste disposal in an argillaceous formation", *J. Rock Mech. Geotech. Eng.*, **5**(1), 277-286.

Loschetter, A., Smaï, F., Sy, S., Burnol, A., Leynet, A., Lafortune, S. and Thoraval, A. (2012), "Simulation of CO_2 storage in coal seams: Coupling of TOUGH2 with the solver for mechanics CODE_ASTER®", *Proceedings of the TOUGH Symposium 2012*, LBNL, Berkeley, California, U.S.A.

Magri, F., Tillner, E., Jolie, E., Kempka, T., Kolditz, O., Moeck, I., Wang, W., Watanabe, N. and Zimmermann, G. (2012), "3D numerical simulation of pore pressure and stress coupling for CO_2 storage in deep saline aquifers: A case study from the Northeast German Basin", *Geophys. Res. Abstr.*, **14**, EGU2012-3548.

Pandey, S.N., Chaudhuri, A. and Kelkar, S. (2017), "A coupled thermo-hydro-mechanical modeling of fracture aperture alteration and reservoir deformation during heat extraction from a geothermal reservoir", *Geothermics*, **65**, 17-31.

Pruess, K., Oldenburg, C. and Moridis, G. (1999), *TOUGH2 User's Guide, V2.0*, Lawrence Berkeley National Laboratory Report LBNL-43134, Berkeley, California, U.S.A.

Rutqvist, J. and Tsang, C.F. (2003), "TOUGH-FLAC: A numerical simulator for analysis of coupled thermal-hydrologic-mechanical processes in fractured and porous geological media

under multi-phase flow conditions", *Proceedings of the TOUGH Symposium 2003*, Berkeley, California, U.S.A., May.

Rutqvist, J. and Tsang, C.F. (2002), "A study of caprock hydromechanical changes associated with CO_2-injection into a brine formation", *Environ*. *Geol*., **42**(2-3), 296-305.

Rutqvist, J. and Moridis, G.J. (2008), D*evelopment of a Numerical Simulator for Analyzing the Geomechanical Performance of Hydrate-Bearing Sediments*, Report Number: LBNL-467E.

Rutqvist, J., Vasco, D.W. and Myer, L. (2010), "Coupled reservoir-geomechanical analysis of CO_2 injection and ground deformations at In Salah Algeria", *Int*. *J*. *Greenhouse Gas Control*, **4**(2), 225-230.

Rutqvist, J. (2011), "Status of the TOUGH-FLAC simulator and recent applications related to coupled fluid flow and crustal deformations", *Comput*. *Geosci*., **37**(6), 739-750.

Shahrbanouzadeh, M., Barani, G.A. and Shojaee, S. (2015), "Analysis of flow through dam foundation by FEM and ANN models Case study: Shahid Abbaspour Dam", *Geomech*. *Eng*., **9**(4), 465-481.

Stephen, W.W. (2011), *EOS7C-ECBM Version 1.0: Additions for Enhanced Coal Bed Methane Including the Dusty Gas Model*, Canyon Ridge Consulting Report CRC2011-0002, Sandia Park, New Mexico, U.S.A.

Sugita Y., Maßmann, J., Pan, P., Rutqvist, J. and Kwon, S. (2015), "Problem definition, team structure, achievement and issues Task 2, Decovalex-2015 project", *Proceedings of the 7th DECOVALEX-2015 Workshop*, Wakkanai, Horonobe, Japan.

Tong F., Jing, L. and Zimmerman, R.W. (2010), "A fully coupled thermos-hydro-mechanical model for simulating multiphase flow, deformation and heat transfer in buffer material and rock masses", *Int*. *J*. *Rock Mech*. *Min*. *Sci*., **47**, 205-217.

Watanabe, N., McDermott, C.I., Wang, W., Taniguchi, T. and Kolditz, O. (2009), "Sensitivity analysis of thermo-hydro-mechanical(THM) coupled processes in a hot-dry-rock reservoir", *Proceedings of the 34th Workshop on Geothermal Reservoir Engineering*, Stanford, California, U.S.A., February.

Yang, J., Chen, L., Liao, H. and Yang, F. (2013), "Simulation on THM coupling process of deep rock roadway with aquifer in coalmine", *Adv*. *Mater*. *Res*., **671-674**, 1131-1134

Yildizdag, K. (2010), *THM Modelling Manual of a 2D Tunnel for Disposal of Waste Repositories: Computed Thermal,Hydraulic and Mechanic Response of a 2D Axis-symmetric Tunnel Performed by the Software GeoSys/RockFlow*, Lambert Academic Publishing.

GC